EITN90 Radar and Remote Sensing
Lecture 13: Remote sensing

Daniel Sjöberg

Department of Electrical and Information Technology

Spring 2020

Lunch lectures at Axis Communications tomorrow

- Wednesday March 4.
- 12:55 Meet at Axis reception.
- 13:00 Radar lectures with speakers from industry, meeting room Keops.

The lunch and the lectures are held at Axis Communications AB in Lund. It is at the main Axis building at Emdalavägen 14 (15 minute walk from LTH). First go to the reception.

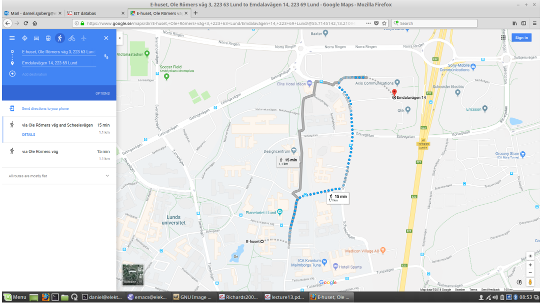

Learning outcomes of this lecture

In this lecture we will

- See how radar systems can provide earth observation data.
- Observe how different surface structure and materials affect reflection properties.
- Understand the difference between active and passive sensing.

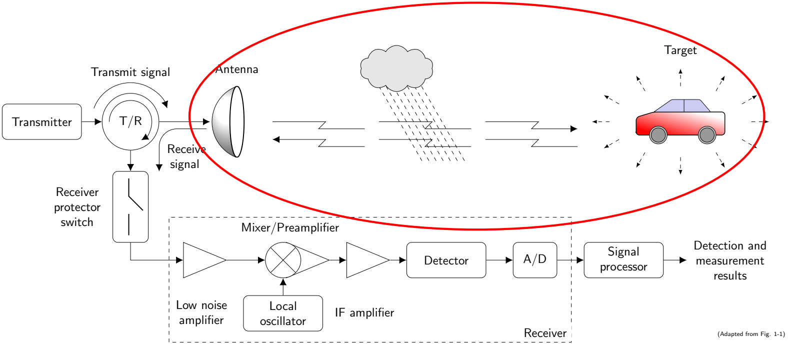

Outline

1. **General features of remote sensing**
2. **Scattering from earth surface features**
3. **Passive microwave imaging**
4. **Conclusions**

Outline

What is remote sensing?

- Acquiring information about an object or feature without physical contact.
- Most often from a satellite or aircraft platform.
- Active or passive sensing possible.
- Optical regime gives high resolution but is sensitive to weather conditions.
- Microwaves have less resolution but good penetration.
- Earth observation over time provides global data, giving climate information.

Satellite orbits to scale

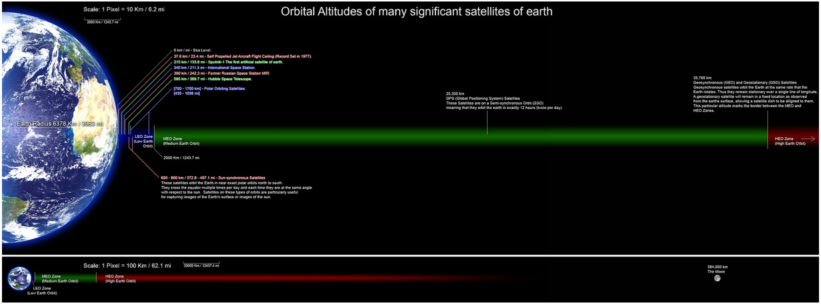

By Rrakanishu - Own work, GFDL, https://commons.wikimedia.org/w/index.php?curid=4189737

Earth observation satellites usually in Low Earth Orbit (LEO), around 800 km.

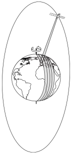

LEO

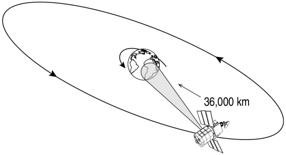

GEO

Opacity of the atmosphere

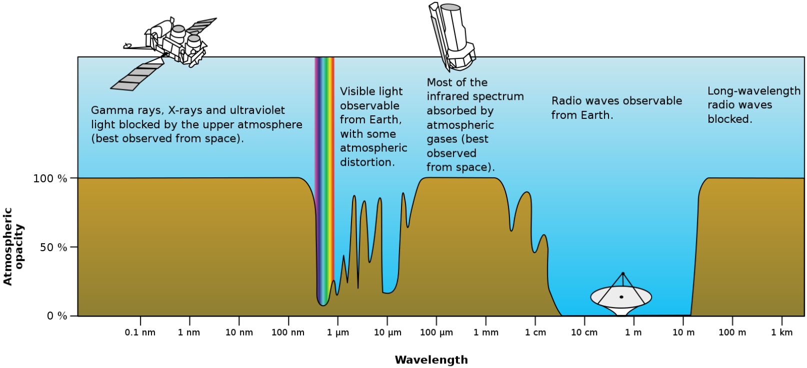

(Figure originally by NASA)

Windows of transparency are available in the electromagnetic spectrum.

Zoomable satellite images

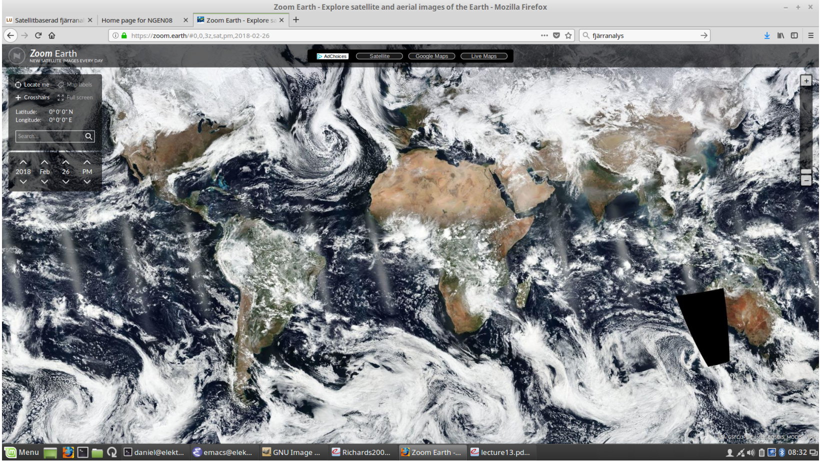

https://zoom.earth, https://satellites.pro,
https://earth.google.com. . .

Example of data: Weather

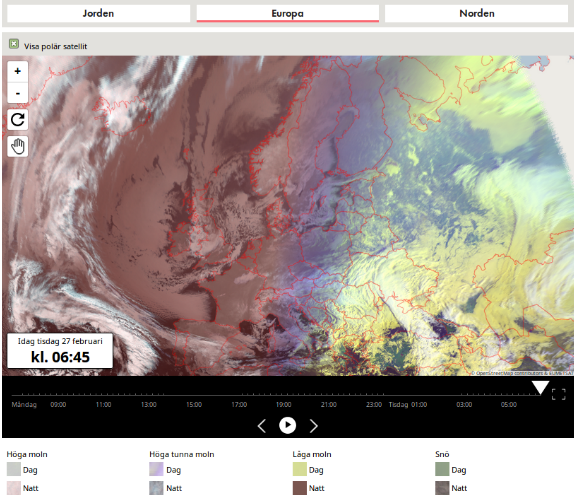

Data available from SMHI, composite image from several satellites and wavelengths.

Outline

Scattering mechanisms

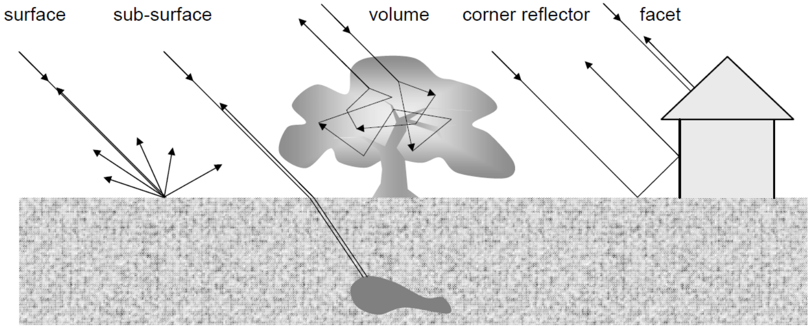

Fig. 5.1. Common scattering mechanisms

Scattering occurs due to many different features.

Fresnel coefficients

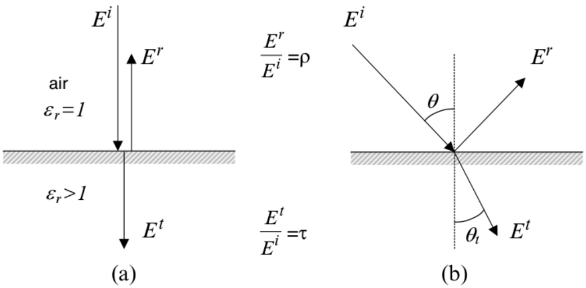

Fig. 5.2. Definition of reflection and transmission coefficients (a) vertical incidence and (b) oblique incidence

$$\rho_\mathrm{H} = \frac{\cos\theta - \sqrt{\epsilon_\mathrm{r} - \sin^2\theta}}{\cos\theta + \sqrt{\epsilon_\mathrm{r} - \sin^2\theta}}$$

$$\rho_\mathrm{V} = \frac{-\epsilon_\mathrm{r}\cos\theta + \sqrt{\epsilon_\mathrm{r} - \sin^2\theta}}{\epsilon_\mathrm{r}\cos\theta + \sqrt{\epsilon_\mathrm{r} - \sin^2\theta}}$$

Reflectance is $\Gamma = |\rho|^2$. Material ϵ_r, angle of incidence θ.

Reflection from a rough surface

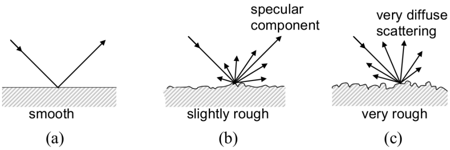

Fig. 5.4. Depicting the trend to diffuse surface scattering as roughness increases

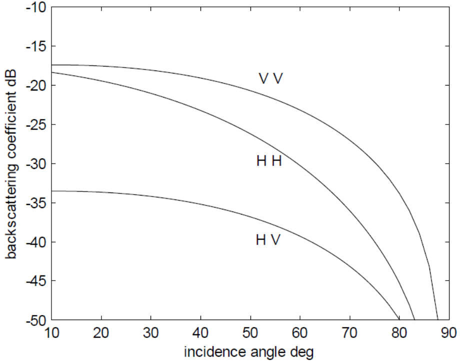

$$\sigma^{o}_{VV}(\theta) = \frac{g\cos^{3}\theta}{\sqrt{p}}\{|\rho_V|^2 + |\rho_H|^2\}$$

$$g = 0.7\{1 - \exp[-0.65(k\mathrm{s})^{1.8}]\}$$

$$\sigma^{o}_{HH}(\theta) = p\sigma^{o}_{VV}(\theta)$$

$$\sigma^{o}_{HV}(\theta) = q\sigma^{o}_{VV}(\theta)$$

$$p = \left[1 - \left(\frac{2\theta}{\pi}\right)^{0.33/|\rho(0)|^2}\exp(-k\mathrm{s})\right]^2$$

$$q = 0.23|\rho(0)|[1 - \exp(-k\mathrm{s})]$$

Fig. 5.6. Demonstration of the differences in horizontal and vertical polarisation responses for a rough surface, and an illustration of typical cross-polarised scattering; generated using the semi-empirical model

Cross-polarized ratio

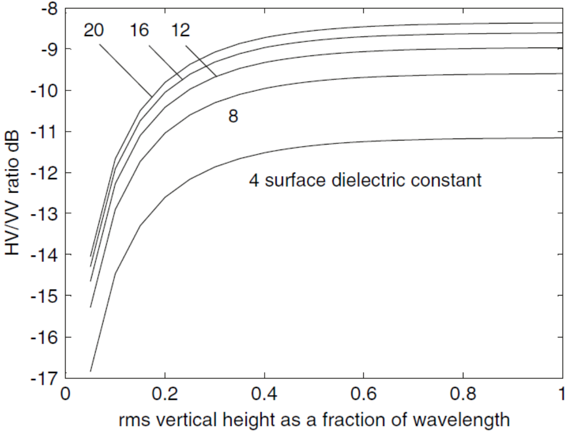

Fig. 5.7. The cross polar ratio as a function of surface roughness and dielectric constant; the dependence on surface moisture content can be determined by referring to relationships such as that in Fig. 5.3 for sand

Co-polarised ratio: almost equal

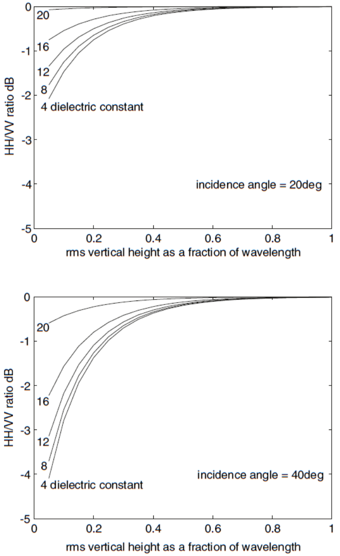

Fig.5.8. The co-polarised ratio as a function of surface roughness and dielectric constant for two values of incidence angle

Co-polarized backscattering, absolute values

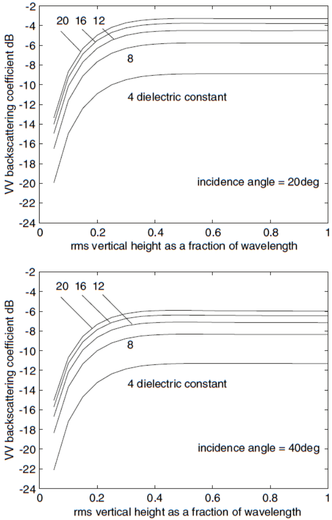

Fig. 5.9. The vertically polarised surface backscattering coefficient as a function of surface roughness and surface dielectric constant for two angles of incidence

Penetration depth vs moisture content

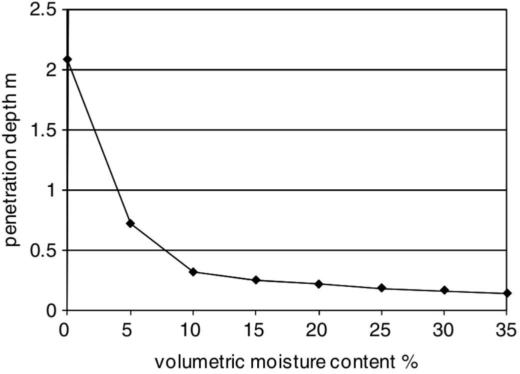

Fig. 5.13. Penetration depth for sand as a function of moisture content at L band, with a wavelength of 23.5cm

$$\delta \approx \frac{\lambda}{2\pi}\frac{\sqrt{\epsilon_r'}}{\epsilon_r''}, \quad \epsilon_{rc} = \epsilon_r' - j\epsilon_r''$$

Moisture: infrared vs microwave

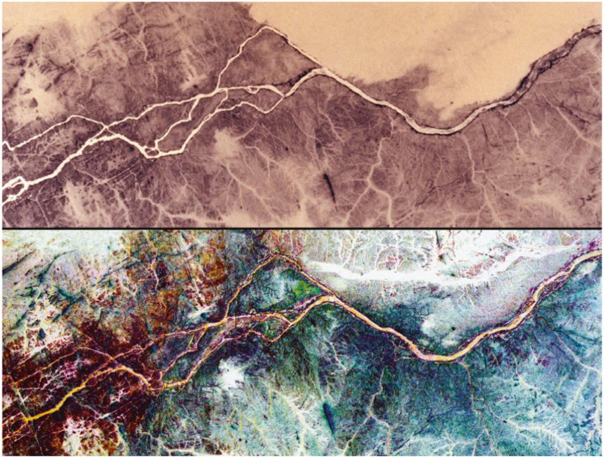

Fig. 5.14. Colour infrared photograph (top) and SIR-C radar image (bottom) recorded in 1995 over the Sahara Desert in Sudan. In the top right hand quadrant of the radar image a previous, ancient channel of the Nile is evident, now buried under sand; the colour composite radar image was created by displaying the C band VH cross-polar channel as red, the L band VH cross-polar channel as green and the L band co-polar HH channel as blue; since the paleo channel appears white there is good penetration at each of those wavelength/polarisation combinations (image courtesy of NASA JPL)

Effects from multiple reflections

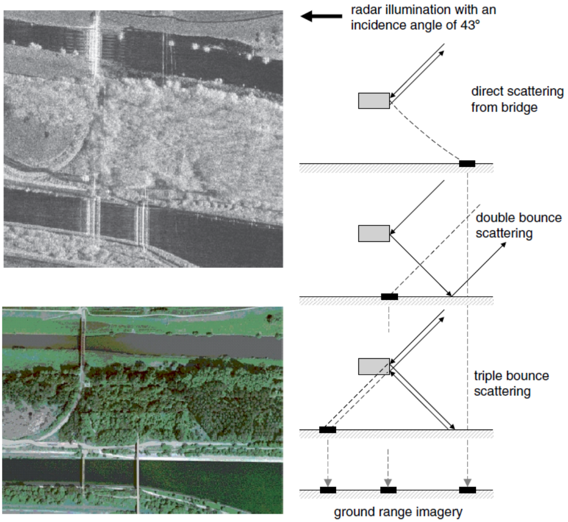

Fig. 5.24. Typical scattering from a bridge, showing how multiple reflections are formed; the imagery was taken by permission from U. Soergel, A. Thiele, H. Gross and U. Thoennessen, Extraction of bridge features from high-resolution InSAR data and optical Image", *2007 Urban Remote Sensing Joint Event*, Paris ©2007 IEEE

Strong return from orthogonal structures

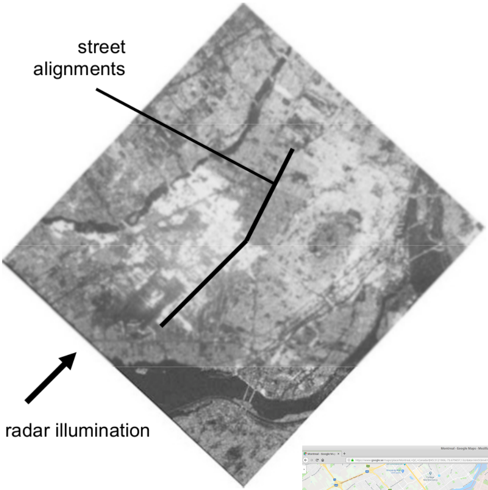

Fig. 5.30. Portion of a SIR-B image acquired over Montreal, Canada demonstrating the cardinal effect; the bright central portion of the image is where cross streets are aligned orthogonally to the incoming radar energy, whereas the portions to the north, of about the same urban density, have street patterns not orthogonal to the radar beam (from J.P. Ford, J.B. Cimino, B. Holt and M.R. Ruzek, *Shuttle Imaging Radar Views the Earth From Challenger: the SIR-B Experiment,* JPL Publication 86-10, NASA, 15 March 1986)

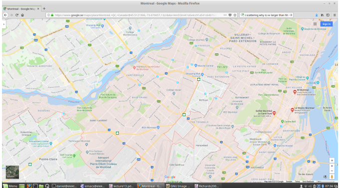

Composite scatterers

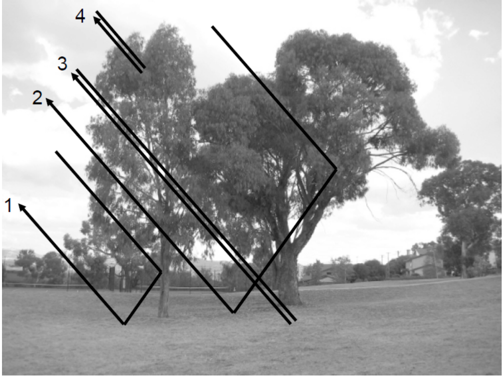

Fig. 5.31. Typical scattering pathways for trees and forest stands: 1 is trunk-ground corner reflector scattering; 2 is canopy-ground scattering, 3 is scattering from the ground after transmission through the canopy and 4 is canopy volume scattering

Different scattering pathways may add coherently or incoherently. With a large number of randomly placed scatterers, incoherent addition (adding RCS) is a reasonable assumption.

Sea surface scattering: angle of incidence

20°

(a)

40°

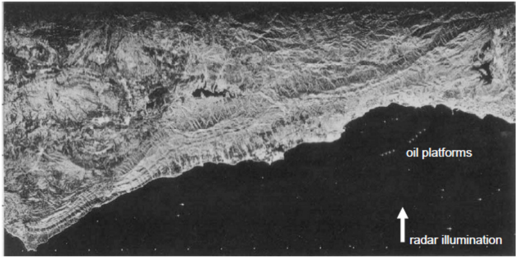

(b)

Fig. 5.34. Seasat mosaic (a) and SIR-A (b) image of the coastal region around Santa Barbara, California (from J.P. Ford, J.B. Cimino and C. Elachi, *Space Shuttle Columbia Views the World With Imaging Radar: the SIR-A Experiment*, JPL Publication 82-95, NASA, 1 January 1983)

Different ages of ice show up in different frequencies

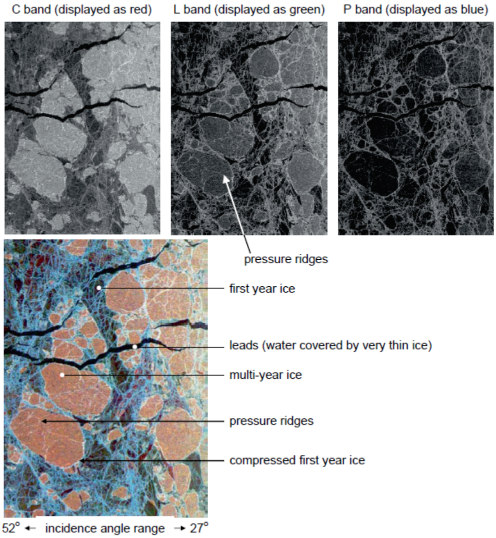

Fig. 5.39. Multi-wavelength aircraft SAR imagery of sea ice (from B. Scheuchl, I. Hajnsek and I. Cumming, Classification strategies for polarimetric SAR sea ice data, *Workshop on Applications of SAR Polarimetry and Polarimetric Interferometry*, Frascati, Italy, 14-16 January 2003, ©2003 ESA/ESRIN)

Outline

Passive microwave energy available

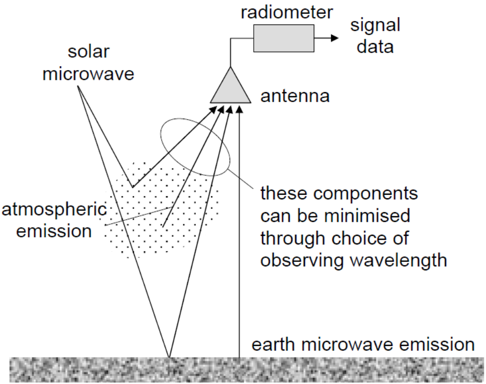

Fig. 9.1. The components of passive microwave energy theoretically available for measurement

Passive technology means no SAR is possible. Pixel sizes on the order of 10 km.

Radiometric brightness temperature

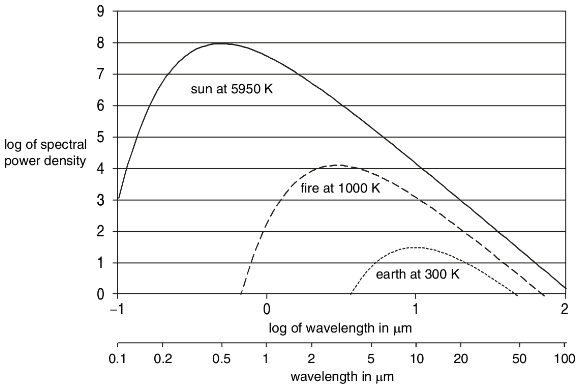

Fig. 2.2. Spectral power density available for ideal black bodies at three different temperatures, computed from (2.2)

Power received in bandwidth B from a surface at temperature T is

$$P_{\mathrm{r}} = \varepsilon k T B = k T_{\mathrm{B}} B, \quad \text{where} \quad T_{\mathrm{B}} = \varepsilon T = \frac{P_{\mathrm{r}}}{kB}$$

and $\varepsilon \leq 1$ is the emissivity of the surface.

Infrared vs microwave: sea surface temperature

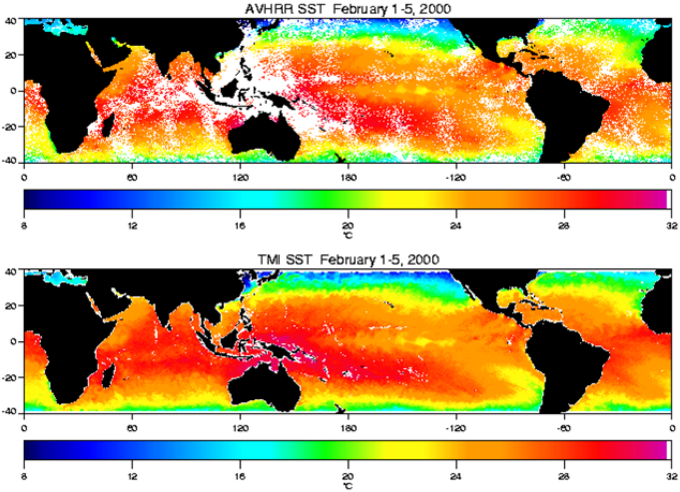

(http://www2.hawaii.edu/ jmaurer/sst/)

Top: infrared, bottom: microwaves. Microwaves penetrate clouds more easily.

Passive Microwave Remote Sensing Techniques for Studying Climate

Absorptivity and reflectivity

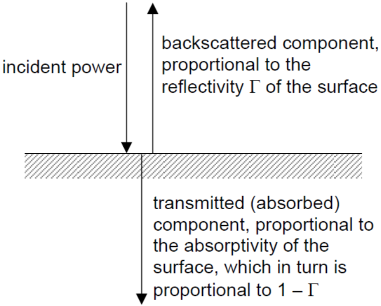

Fig. 9.2. Relationship between the absorptivity and reflectivity of a surface

At thermal equilibrium, emitted power must be equal to absorbed power, or

$$\varepsilon = 1 - \Gamma$$

where Γ is the reflectivity (power measure). Note that a highly reflective surface ($\Gamma \approx 1$) has low emissivity, $\varepsilon \approx 0 \Rightarrow T_\mathrm{B} \approx 0$. Hence, metal surfaces appear as black in passive sensing.

Rough surface

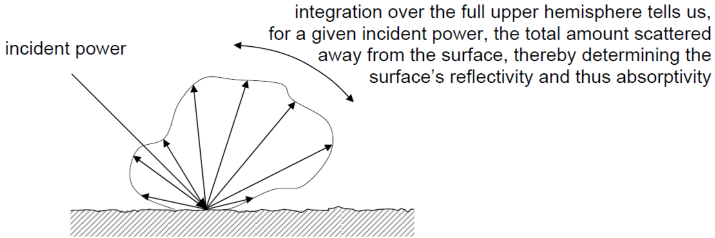

Fig. 9.3. All the power scattered into the upper hemisphere has to be found when determining reflectivity for a rough surface

For rough surfaces, the reflectivity Γ must correspond to power reflected in all directions.

Brewster angle

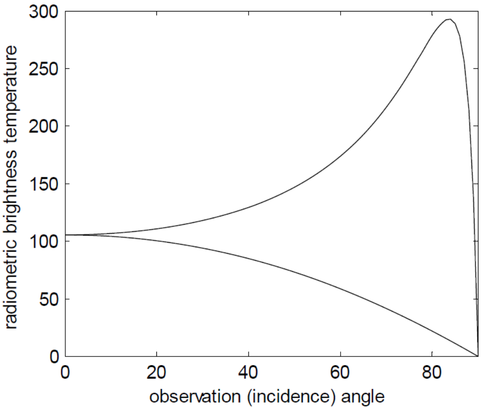

Fig. 9.4. Radiometric brightness temperature for still water as a function of observation angle and polarisation

At the Brewster angle for a smooth surface (like still water), there is zero reflection of vertical polarization, hence large emissivity corresponding to physical temperature.

Brightness of different surfaces

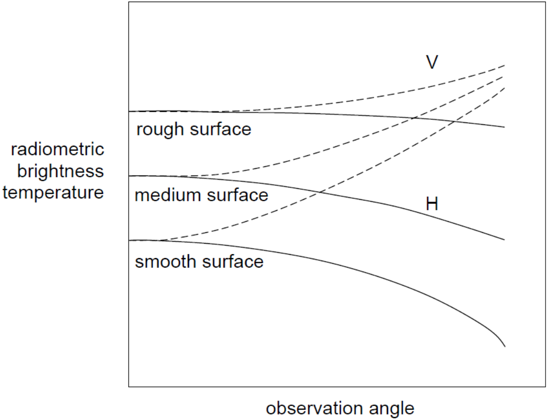

Fig. 9.6. Dependence of radiometric brightness temperature on surface roughness and polarisation

Example: smooth sand with different moisture

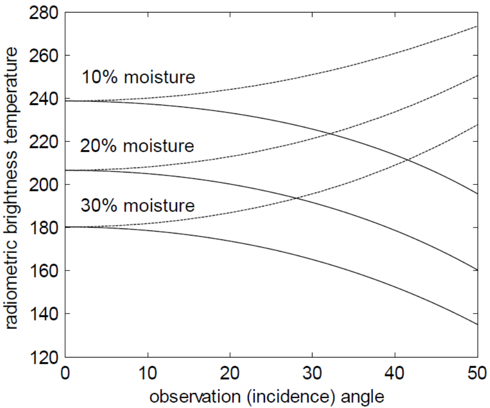

Fig. 9.8. Computed radiometric brightness temperature of smooth sand at 1.4GHz as a function of moisture content using the dielectric constants of Table 9.1, ignoring the effect of the (small) imaginary component of the dielectric constant and any surface roughness; the full lines represent horizontal polarisation and the dotted (upper) lines vertical polarisation

Soil Moisture Active Passive (SMAP)

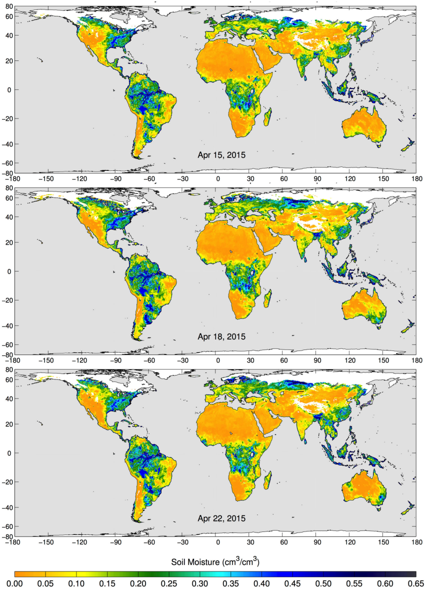

Soil Moisture Active Passive (SMAP)

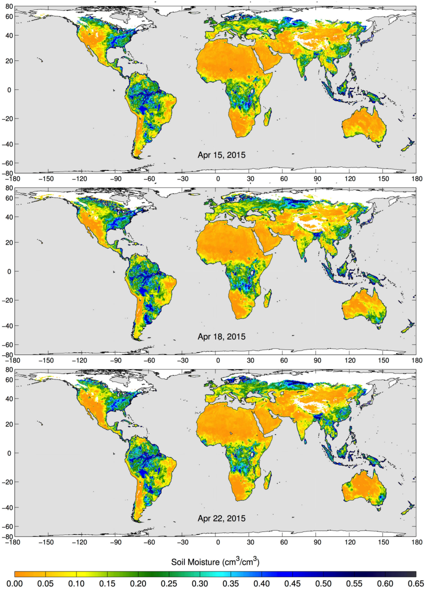

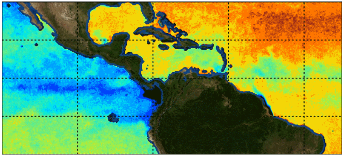

Typical range of brightness temperature

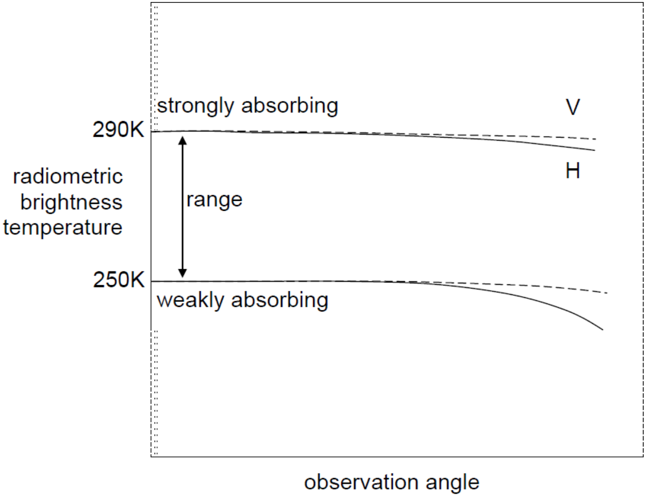

Fig. 9.9. Likely range of radiometric brightness temperatures for a volume medium

Passive microwave sensing of the atmosphere

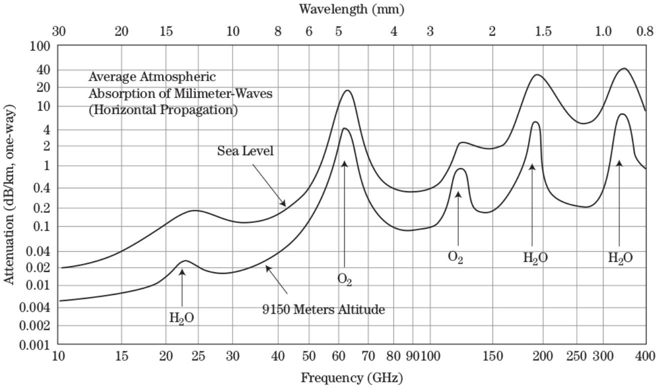

FIGURE 1-13 One-way atmospheric attenuation as a function of frequency at sea level and at 9150 meters altitude. (From U. S. Government work.)

(Figure from POMR)

Due to thermal equilibrium, the atmosphere will have strong emission in the absorption bands. In order to detect atmospheric content with a passive sensor, frequency can be chosen corresponding to absorption peaks.

Putting it all together: the carbon cycle (ESA)

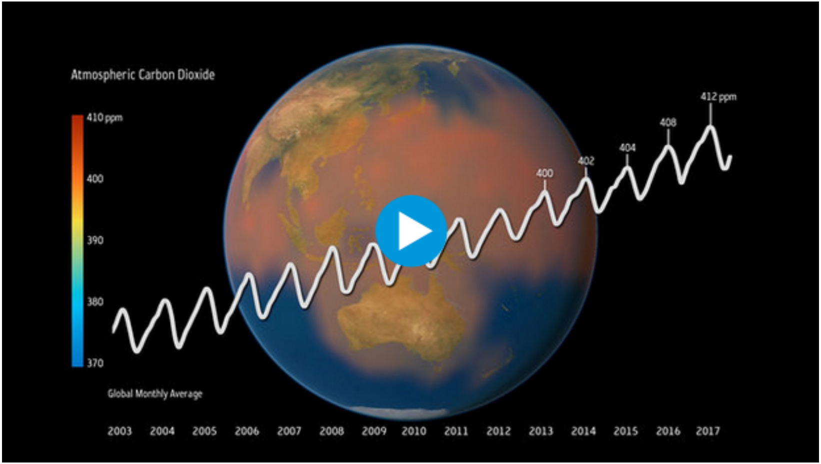

As part of the way Earth works as a system, carbon is continuously passed between the ocean, the land and the atmosphere. This involves a range of different processes, some of which can be observed by satellites. Human activity is disturbing these natural processes and causing a rise in atmospheric carbon dioxide. Satellites and ESA's Climate Change Initiative are helping to improve our understanding of the carbon cycle and its role in climate change. [https://earth.esa.int/web/guest/content/-/article/carbon-cycle]

Outline

Conclusions

- Remote sensing provides possibilities for long time earth observation, facilitating data for climate observations.
- Active sensors use radar/lidar techniques, high resolution.
- Passive sensors detect the brightness temperature of the scene, low resolution.